Aerosol Science and Technology

Toward Developing A New Occupational Exposure Metric Approach for Characterization of Diesel Aerosols

Emanuele G. Cauda [a], Bon Ki Ku [b], Arthur L. Miller [a] & Teresa L. Barone [c]

[a] U.S. Department of Health and Human Services, Public Health Service, Centers for Disease Control and Prevention, National Institute for Occupational Safety and Health, Office of Mining Safety and Health Research, Pittsburgh, Pennsylvania, USA

[b] U.S. Department of Health and Human Services, Public Health Service, Centers for Disease Control and Prevention, National Institute for Occupational Safety and Health, Division of Applied Research and Technology, Cincinnati, Ohio, USA

[c] Emissions and Catalysts Research Center, Oak Ridge National Laboratory, Knoxville, Tennessee, USA

PLEASE SCROLL DOWN FOR ARTICLE

Toward Developing a New Occupational Exposure Metric Approach for Characterization of Diesel Aerosols

Emanuele G. Cauda,[1] Bon Ki Ku,[2] Arthur L. Miller,[1] and Teresa L. Barone[3]

[1]*U.S. Department of Health and Human Services, Public Health Service, Centers for Disease Control and Prevention, National Institute for Occupational Safety and Health, Office of Mining Safety and Health Research, Pittsburgh, Pennsylvania, USA*

[2]*U.S. Department of Health and Human Services, Public Health Service, Centers for Disease Control and Prevention, National Institute for Occupational Safety and Health, Division of Applied Research and Technology, Cincinnati, Ohio, USA*

[3]*Emissions and Catalysts Research Center, Oak Ridge National Laboratory, Knoxville, Tennessee, USA*

The extensive use of diesel-powered equipment in mines makes the exposure to diesel aerosols a serious occupational issue. The exposure metric currently used in U.S. underground noncoal mines is based on the measurement of total carbon (TC) and elemental carbon (EC) mass concentration in the air. Recent toxicological evidence suggests that the measurement of mass concentration is not sufficient to correlate ultrafine aerosol exposure with health effects. This urges the evaluation of alternative measurements. In this study, the current exposure metric and two additional metrics, the surface area and the total number concentration, were evaluated by conducting simultaneous measurements of diesel ultrafine aerosols in a laboratory setting. The results showed that the surface area and total number concentration of the particles per unit of mass varied substantially with the engine operating condition. The specific surface area (SSA) and specific number concentration (SNC) normalized with TC varied two and five times, respectively. This implies that miners, whose exposure is measured only as TC, might be exposed to an unknown variable number concentration of diesel particles and commensurate particle surface area. Taken separately, mass, surface area, and number concentration did not completely characterize the aerosols. A comprehensive assessment of diesel aerosol exposure should include all of these elements, but the use of laboratory instruments in underground mines is generally impracticable. The article proposes a new approach to solve this problem. Using SSA and SNC calculated from field-type measurements, the evaluation of additional physical properties can be obtained by using the proposed approach.

[Supplementary materials are available for this article. Go to the publisher's online edition of *Aerosol Science and Technology* to view the free supplementary files.]

INTRODUCTION

The relationship between aerosol exposure and health effects in occupational environments has been extensively investigated and reviewed. Crucial steps for studying this relationship include evaluating occupational aerosols via measurement and characterization techniques. One of the goals of the National Institute for Occupational Safety and Health (NIOSH) is to reduce work-related illness by generating and promoting new scientific knowledge. Whereas through the first part of the 20th century, particle number was the primary metric for determining health-related aerosol exposure risk (Walton and Vincent 1998), in the last 50 years risk has been mostly characterized in terms of mass concentration of the particles (Maynard and Jensen 2001; Maynard and Aitken 2007).

The use of aerosol mass concentration as a metric has recently been questioned and challenged, in particular because of the rapid increase of the nanotechnology sector and the related exposure of the workers to ultrafine or nanoscale particles (mean diameter smaller than 0.1 μm) (Balbus et al. 2007). Among aerosol and nanotoxicology scientists, there is still considerable uncertainty over which method should be employed to characterize ultrafine and nanoaerosol exposures, but there is gathering consensus that relying only on mass concentration measurements will clearly not be appropriate (Maynard and Kuempel 2005; Oberdorster et al. 2005; Wittmaack 2007; Sager et al.

The mention of any company or product does not constitute an endorsement by the National Institute for Occupational Safety and Health (NIOSH). The findings and conclusions in this article are those of the authors and do not necessarily represent the views of NIOSH.

Address correspondence to Emanuele G. Cauda, U.S. Department of Health and Human Services, Public Health Service, Centers for Disease Control and Prevention, National Institute for Occupational Safety and Health, Office of Mining Safety and Health Research, 626 Cochrans Mill Road, Pittsburgh, PA 15236, USA. E-mail: ecauda@cdc.gov

2008; Pauluhn 2009; Fubini et al. 2010; Schulte et al. 2010). To address this issue, a recent publication presented an overview of four different metrics (number, length, surface area, mass) to evaluate aerosol exposure with reference to various classes or attributes of nanostructured particles (Maynard and Aitken 2007). Based on that work, it appears that particle surface area may be an appropriate metric for characterizing nanoscale materials. This approach is also supported by data suggesting a correlation between particle surface area and inflammatory response for different materials (Karakoti et al. 2006; Sager et al. 2008; Sager and Castranova 2009), and other data showing strong toxicity-based evidence that surface area is an appropriate exposure metric for low solubility particles (Tran et al. 2000; Brown et al. 2001.; Monteiller et al. 2007; Sager et al. 2008).

While measurement of ultrafine aerosol particle number concentration requires an understanding of instrument range of operability, accuracy, and calibration, the study of the aerosol surface area leads to more complex challenges, herein described. The Brunauer–Emmett–Teller (BET) method (Brunauer et al. 1938), the standard method for measuring the total exposed surface area of particles, is based on the adsorption of gas molecules on the surface of the particles. This method, which is generally used to characterize bulk material like powders, is only available as off-line analysis and requires a large mass of sample.

Several real-time techniques for estimating the surface area have been evaluated, all of them using principles different from gas adsorption. Monitors using the diffusion charging technique have been found to be capable of measuring the active surface area of ultrafine particles (Ntziachristos et al. 2004; Jung and Kittelson 2005; Ku and Maynard 2005). Active surface area (Fuchs 1963) is defined as the surface of a particle that is involved in interactions with the surrounding gas. The diffusion charging technique is also the basis for a recently developed monitor (Fissan et al. 2007; Wilson et al. 2007), which has the response proportional to the ICRP lung deposition model for the alveolar and tracheobronchial regions of the lung (Fissan et al. 2007). This monitor indicates the aerosol surface area deposited in different regions of the lung for particles up to 400 nm (Asbach et al. 2009). The specific response of the diffusion chargers to a single particle has been found to be affected by the size of the particle (Ku and Maynard 2005; Ku 2010). The size distribution of the aerosol obtained from an electro-mobility analyzer can also be processed to estimate the surface area of the particles (Woo et al. 2001; Ku and Maynard 2005; Lall and Friedlander 2006; Wang and Friedlander 2007). The size distribution measurement, and thus the estimated surface area, is affected by the morphology and aggregation of the particles (Lall and Friedlander 2006) but these are typically not known with precision in occupational environments without in-depth analysis. Studies that compared the results of these methods for measuring the surface area of ultrafine and nanoaerosols have been performed (Ku 2010) and recently concluded (Ku and Kulkarni 2012).

The toxicological studies on occupational ultrafine particles generally do not consider how the aerosols are monitored and measured in the field. Since the proponents of using surface area as a metric for nanoparticles exposure have so far not provided indication on which type of surface area is the most appropriate, it is advisable to use as many different measurement methods as possible. The feasibility of the measurements on site needs to be considered too: some monitors can be easily employed in field studies (diffusion chargers), while the complexity, size, and lack of robustness of electro-mobility spectrometers complicate their use in environments different than laboratories.

In underground mines, diesel-powered equipment emissions are the main contributor to ultrafine aerosol, generally referred to as diesel particulate matter (DPM). The International Agency for Research on Cancer (IARC) has labeled diesel exhaust as a human carcinogen (Benbrahim-Tallaa et al. 2012) while the National Institute for Occupational Safety and Health (NIOSH) (NIOSH and CDC 1988) has identified DPM as a potential occupational carcinogen. Deployment of contemporary (cleaner) diesel engines along with exhaust aftertreatment technologies such as diesel particulate filter (DPF) systems, disposable filter elements (DFEs), diesel oxidation catalysts (DOCs), and the use of alternative fuels such as biodiesel, are commonly considered the most effective strategies and technologies for curtailing DPM at its source.

Recent studies have shown that these strategies can effectively limit the DPM aerosol mass concentration to the permissible exposure level (Bugarski et al. 2006, 2009). The same studies, which focused the impact of uncatalyzed DPFs on emissions, showed how the average size of the aerosol measured in the mine atmosphere by an electro-mobility spectrometer shifts toward smaller particles (Bugarski et al. 2006, 2009): likely the post-DPF aerosol measured was mainly formed by nucleation of semivolatile compounds with a different chemical composition from the original emitted DPM, but no definitive data were presented. From a size distribution perspective, the DPM consists of two distinctive modes (Kittelson 1998): an accumulation mode with a median around 100 nm and a nucleation mode characterized by a peak below 30 nm. While the accumulation mode is the predominant mode present for exhaust without aftertreatment technologies, high number concentrations related to nucleation mode have been recorded on treated exhausts.

Currently, the concentration of DPM in underground US noncoal mines is measured by using two surrogates, elemental carbon (EC) and total carbon (TC) carried out via the NIOSH 5040 method. The TC is the carbonaceous portion of the DPM total mass and the EC is the nonorganic portion of TC. The DPM total mass is generally not measured because its results might be affected by nondiesel PM sources present in the mines. Currently, the DPM permissible exposure level in underground noncoal mines is set to a level of 160 μg/m^3 TC and the measurement of EC is carried out regularly (71 Fed. Reg. 28924 2006).

From an occupational exposure perspective, the variability in the DPM urges the assessment in underground mines to be reconsidered. Research is needed to prove if the current metric alone, based on the mass concentration of DPM, is capable of completely characterizing the exposure to this evolving aerosol from a physical perspective. The complexity of the DPM aerosols suggests that a comprehensive assessment should not be limited to the measurement of a single physical property. From a source characterization standpoint, the surface area of DPM nanoparticles emitted by a diesel engine was recently identified as a physical parameter appropriate for evaluating biological response (Ramachandran et al. 2005; Alfoldy, et al. 2009; Giechaskiel et al. 2009; Hesterberg et al. 2010; Swanson et al. 2010). The variability in number concentration of the emitted DPM particles under different engine configurations and operating conditions calls for the evaluation of that property too.

This study is a part of a comprehensive effort to evaluate the exposure assessment in relation to the evolution of DPM aerosol in underground mines, mainly due to the use of aftertreatment technologies and other abatement strategies. As a first step of this effort, the current metric (mass-based) was employed simultaneously with two additional physical metrics—surface area and number concentration—to measure the aerosols emitted by an untreated diesel engine exhaust under three different engine conditions. The tests were carried out in a laboratory exposure chamber, which provides controllable and relatively stable testing conditions. An array of particle measurement systems and methodologies was used to fully analyze the properties of DPM aerosols.

The aim of this study was to explore an approach based on field-feasible measurements of the three metrics in order to generate a more complete characterization of the DPM ultrafine aerosol. Since the complexity of the surface area measurement is of particular interest, special focus was placed on measuring the aerosol surface area using different techniques.

METHODS

Aerosol Generation

A stable source of DPM aerosol was provided using a Marple aerosol chamber (Figure S1–S2 in the online supplemental information) (Marple and Rubow 1983). The chamber is hexagonal in cross section, 2.44-m high with an inside diameter of 1.19 m. Aerosol is introduced at the top of the chamber, is thoroughly mixed by an air jet, and flows through a 10-cm-thick honeycomb structure in which turbulence is reduced and low-velocity flow exits and passes through the test section. Past work has shown the sampling zone of the chambers to be very uniform with relative standard deviation between samples typically less than 0.05 (Marple and Rubow 1983).

The emissions of a Kubota diesel engine connected to a 10-kW electrical generator (constant speed 1800 rpm) were used as a source of DPM aerosol. Diesel electrical generators are very

common in underground mines for power generation. The exhaust of the diesel engine was not retrofitted with any control technology: this configuration is still the common practice for most diesel engines in underground noncoal mines. Previous studies on the engine showed a DPM aerosol very rich in EC and a very low concentration in volatile compounds (Noll and Birch 2008). The engine was run on ultra-low sulfur, road grade diesel fuel. Three resistive load conditions were employed (5, 30, and 80%) to mimic typical working conditions for the engine. The 5% load represents the idle condition whereas the 30% load characterizes a light working condition. A working condition under heavy load is represented by the 80% load. During tests, a portion of the exhaust emitted by the engine was mixed with particle-free fresh air just before the introduction in the Marple chamber. The target was to obtain two mass concentration levels of DPM in the chamber, "low" and "high." Past studies on the chamber showed that the dilution ratio was approximately 200 and 500 for high and low mass concentration, respectively. The low mass concentration level was designed to target a TC concentration below or close to the current permissible exposure limit (160 μg/m^3) in underground noncoal mines, whereas the high mass concentration level targeted TC levels that would be out of compliance in an underground mine (approx. 500 μg/m^3). A tapered element oscillating microbalance, total mass concentration (TEOM 1400a) (Thermo Scientific, Franklin, MA, USA), was used to monitor the DPM aerosol mass concentration in real time. Tests were started when the aerosol concentration in the chamber was steady as measured by the TEOM. The mass concentration was maintained for 4 h to allow the sampling of a representative portion of particles for the real-time monitors and off-line analyses.

Real-Time Measurement

Several real-time monitors were employed in parallel to measure the properties of the aerosol present in the chamber under different testing conditions. Each monitor extracted the aerosol from the Marple chamber via a conductive tube (6-mm OD). A correction for diffusion losses was not considered. The number-weighted particle size distribution of the aerosol was measured with a model 3936 Scanning Mobility Particle Sizer (SMPS) spectrometer (TSI, Shoreview, MN, USA). The concentration of particles from 14.6 to 661 nm was measured with a scanning time of 120 s. The SMPS consisted of a 3080 differential mobility analyzer (DMA) and a 3776 condensation particle counter (CPC), with sample and sheath airflow rates of 0.3 and 3 lpm, respectively. The density was assumed to be constant 1.8 g/cc and the diffusion correction was applied. The SMPS data for both number and surface area were interpreted by using the idealized aggregates (IA) method (Lall and Friedlander 2006), which was previously used for DPM particles emitted by diesel generators (Chung et al. 2008).

The number concentration of the particles was also monitored by a portable CPC (3007, TSI, Shoreview, MN, USA). For some engine conditions, the aerosol concentration in the chamber

exceeded the maximum limit of the portable CPC (which is about 10^5 particles/cm^3). Therefore, a T-valve with a HEPA (high-efficiency particulate arrestor) filter in the clean line, or a dilutor consisting of an HEPA filter cartridge with a single orifice drilled through the end cap (Evans et al. 2010), was used as a dilution system, and the dilution ratio was calculated during preliminary testing.

The mass concentration of the DPM aerosol was monitored in real time by a TEOM 1400 (Thermo Scientific, Franklin, MA, USA) preceded by a 10-mm Dorr-Oliver cyclone and a DPM cassette impactor (SKC, Eighty Four, PA, USA). The cyclone and impactor preclassified the aerosol entering the TEOM, allowing only particles with an average aerodynamic diameter smaller than 0.8 μm to reach the analyzer (Noll et al. 2005).

A nanoparticle surface area monitor (NSAM, TSI model 3550) was used to measure aerosol surface area concentrations that would deposit in the alveolar region of the lung. This monitor has been found to provide reliable results even at concentrations above 10^6 #/cm^3 (Asbach et al. 2009). The monitor is equipped with a 1-μm cyclone preselector.

Two portable DC2000CE diffusion charger monitors (DC1, DC2; EcoChem, USA) were used to measure DPM particle active surface area. Both instruments had a manufacturer-specified range of 0–2000 μm^2/cm^3 and sensitivity of 1 μm^2/cm^3. In the diffusion chargers, the sampled aerosol is exposed to a positive ion cloud before collection on a filter and charge measurement.

Sampling for Off-Line Analysis

During each test, a portion of the aerosol present in the Marple chamber was collected on three 37-mm quartz fiber filters for off-line thermo-optical analysis using a commercial DPM sampler (225–317, SKC Inc., Eighty Four, PA, USA). The sampling system included a 10-mm Dorr-Oliver respirable cyclone and an impactor with a cut point of 0.8 μm. Stable flow was maintained using critical orifices connected in line with each sample. To simulate the collection of DPM samples in an underground environment for 8 h while completing a test in four hours, the flow rate was set at 3.4 lpm (twice the usual 1.7 lpm). The higher flow rate changed the sampler cut point, but the concentration of particles larger than 0.4 μm is very low and similar for the three engine conditions (Figure 1). For this reason, the change in the cut is not significant for this study. Each flow rate was checked with an electronic bubble meter (Gilibrator, Gilian Instrument Corp., Wayne, NJ, USA) prior to sampling in every phase of the study. Using a similar sampling system, three TX40 filters (Pall, Ann Arbor, MI, USA) were used to collect samples for the BET analysis during the tests at high mass concentration level.

Samples were collected electrostatically for transmission electron microscopy (TEM) analysis using a beta version of the ESPnano Model 100 particle sampler (ESPnano.com, Spokane, WA, USA) (Miller et al. 2010).The sampler drew aerosol from the Marple chamber at a flow rate of 0.11 lpm. Several times during each test, the sampling tube was purged for 85 s followed

FIG. 1. Mean particle size distribution of DPM aerosols generated in the Marple chamber under three engine load conditions (5, 30, and 80%): (a) low mass concentration level; (b) high mass concentration level. (Color figure available online.)

by a collection time of 10–50 s to extract a representative sample of aerosol. Particles were collected on a 400 mesh copper TEM grid coated with carbon film and were analyzed using a JEOL 2010J Analytical TEM at 2.5×10^4 magnification. Images were acquired at random locations on the TEM grid, and a qualitative morphology comparison was made for particles generated at 5, 30, and 80% load.

Data Processing

For each test, the real-time mass concentration data obtained from the TEOM monitor were averaged for the entire length of the test. In addition, to increase the data population, five periods of stable concentration were identified for each testing condition and the average mass concentration for each period was calculated. DPM samples collected on quartz fiber filters were analyzed using the NIOSH Method 5040 to determine the TC and EC content (Birch 2002), and the average concentration

of TC and EC aerosol present in the chamber was obtained using the total volume of air that passed through the filter during the test. The determination of TC from underground mine samples is generally obtained by correcting the organic carbon (OC) content via subtraction of the amount found in a secondary filter present in the DPM sampler (Noll and Birch 2008). This correction was applied on the samples collected in this study to correct the absorption of volatile nonparticle OC on the primary filter.

The SMPS measurement of the number-weighted particle size distribution provided information on the geometric mean diameter (GMD), geometric standard deviation of the aerosol, and the total number concentration of the particles in the Marple chamber. The GMD was used to classify the aerosol produced by different engine operating conditions. The surface area of the DPM aerosols was calculated from the SMPS raw data by applying the IA method. The surface area of the particles collected on PVC filters was measured using the Brunauer–Emmett–Teller (BET) standard method (Brunauer et al. 1938). Total particle surface area was estimated from seven point adsorption isotherms collected at relative pressures in the range $p/p_0 = .05$ to .35 using a Quadrasorb-*SI* analyzer (Quantachrome Instruments, Boynton Beach, FL, USA). Each filter was analyzed twice and the results were blank corrected for the background filter surface area.

The active surface area concentration data (nm^2 per unit of air volume—cm^3) of the aerosol obtained from the two diffusion chargers were averaged for the entire length of each test and for the five periods of stable TEOM condition. The same operation was carried out for the raw data provided by the NSAM monitor as for the surface area of the particles deposited in the alveolar region of the lung.

The specific surface area (SSA) of the particles (m^2/g) was calculated using the average mass concentration of the aerosols (TEOM data) and the average surface area concentration from the real-time monitors (NSAM, DC1, DC2, and SMPS). The SSA was obtained for the entire length of each test and for the five periods of stable aerosol concentration. The SSA is often used to characterize solid particles and is a useful parameter for comparing and reconciling the surface area data at each of the two mass concentration levels (low and high). Two additional sets of SSA data were obtained using the TC and EC concentration measurements for each test. While the resulting SSA (TC) and SSA (EC) are generally not found in aerosol surface area

studies, they do quantify the aerosol surface area (m^2) per unit of TC and EC (gram) for the DPM particles at each condition. It is important to remember that TC and EC are the only mass concentration measures currently used for determining DPM exposure in underground U.S. metal/nonmetal mines. Both SSA (TC) and SSA (EC) were calculated from the real-time data for the entire length of each test.

An additional measurement of SSA (m^2/g) was obtained by dividing the total surface area of the DPM particles (BET method) with the measurement of the total mass of DPM present on the sampling filter. This value was obtained by measuring and averaging loaded and blank filter masses. The gravimetric method used for the BET data normalization can be compared to the SSA obtained from the real-time monitors and TEOM mass concentration data.

The total number-weighted particle concentrations in the chamber under different conditions were also normalized with TEOM and TC and EC concentration data. The result, specific number concentration (SNC), provides an indication of the number of particles per gram of total mass, TC, and EC in the aerosol, respectively.

RESULTS

Table 1 summarizes the six test conditions for this study. Three steady-state engine loads (5, 30, and 80%) were applied to the electrical generator. The aerosol emitted by the engine under each engine load was directed into the chamber to generate two mass concentration levels: low and high. The table shows the average mass concentration measured by the real-time TEOM monitor and the relative standard deviation: the variance of the mass concentration was between 10 and 20% during each test. All tests were run for 240 min with the exception of the 80% engine load-low mass concentration test, which was run for only 120 min because of engine malfunctioning.

Figure 1 shows the SMPS average number-size distributions for the aerosols in the Marple chamber over three engine load conditions and two mass concentration levels. For each size bin, the standard deviation of the mean is provided. As the engine load increased, the number concentration distribution shifted to larger particles. The distributions were characterized only by the accumulation mode and there was no indication of nucleation mode: the GMD of the DPM aerosols varied from

TABLE 1
Sampling time and mass concentration of DPM aerosols generated in the Marple chamber during the study

| Engine load | 5% | 30% | 80% | 5% | 30% | 80% |
Mass concentration level	Low	Low	Low	High	High	High
TEOM average [$\mu g/m^3$]	67.5	70.2	118.2	223.1	462.3	494.0
TEOM STDEV [$\mu g/m^3$]	9.9	11.2	24.8	35.6	48.3	65.8
Sampling length [min]	240	240	120	240	240	240

TABLE 2

Mean particle size and number concentration for DPM aerosols generated in the Marple chamber under different conditions

Engine load	5%	30%	80%	5%	30%	80%
Concentration level	Low	Low	Low	High	High	High
Geometric mean diameter [nm]	66.2 ± 1.1	86.6 ± 2.9	135.1 ± 4.9	66.9 ± 1.1	92.7 ± 3.6	129.6 ± 3.2
Geometric standard deviation	1.59	1.59	1.66	1.56	1.63	1.66
Total number concentration [10^4 #/cm^3]	23.3 ± 3.8	12.5 ± 2.4	8.1 ± 1.7	65.1 ± 8.2	69.3 ± 5.6	31.1 ± 3.9

66 to 135 nm and the geometric standard deviation was below 1.7 for all the conditions (Table 2). The geometric standard deviations were all in agreement with the DPM aerosol standard deviation proposed by Harris and Maricq (2001). There was no substantial variation in the GMD for aerosols generated by the same engine load when the chamber was operated under low and high mass concentration, which suggests that the dilution of the chamber did not alter the size characteristics of the aerosol. The total number concentration of the particles ranged from 8.1×10^4 to 69.3×10^4 particles/cm^3 and the variation within each test was between 10 and 15%.

The morphology of particles present in the Marple chamber was qualitatively compared for engine loads 5, 30, and 80%. Although a systematic evaluation of particle morphology was not carried out, some images were consistent with the SMPS results. These showed increasing particle size with increasing engine load (Figure 2), which is a relationship reported earlier by Kittelson (1998) in a review of several diesel engine studies. The particles were present as solid nanoparticle aggregates. A preliminary estimation of the primary particle showed a diameter of 25 nm. This value is in line with the literature (Park et al. 2004; Mathis et al. 2005) and it was used to implement the IA method for the SMPS raw data by using the Aerosol Instrument Management (TSI, Shoreview, MN, USA) software tool.

The SSA of the DPM aerosols was calculated by normalizing each instrument measurement with the TEOM mass concentration (Figure 3). The SSA data were plotted against the aerosol GMD characteristic of each engine operating condition. For each condition, the SSA values obtained from the SMPS data were higher than the SSA data obtained from the diffusion charger monitors and the NSAM. While the SSA provided by the BET analysis presented a very scattered trend, the replicate of each sample showed a low standard deviation. The high variance can be attributed to the uncertainties of the sampling process or most probably to the interaction of DPM particles and filter media, which limits the study of surface area with this protocol. Nevertheless, the SSA measured via the BET technique was between the values obtained using two types of real-time monitors. The plots of SSA normalized by TC and EC are provided in the supplemental information (Figure S3).

Table 3 summarizes the surface area concentration and mass concentration of the aerosols measured by real-time monitors and off-line analysis. For each testing condition, the average and standard deviation of the data relative to the whole test were reported in the table. The data from DC1 for all high mass concentration tests and the data from DC2 for a single high mass concentration level at 80% engine load were excluded because of malfunctioning of the monitors.

Independently from the unit used for the mass normalization (TEOM, TC, and EC) or the monitor employed, the SSA was found to decrease as engine load increased from 5 to 80%. For example, the SSA measured by the SMPS and normalized by the TC concentration varied from 80.7–115.3 m^2/g (5%) to 51.2–57.4 m^2/g (80%), while for the NSAM data, the trend was from 17–31 m^2/g (5%) to 8–10 m^2/g (80%). The SSA values obtained using the SMPS data were constantly higher compared to those determined by other monitors or techniques. No substantial difference was found for the SSA data obtained from the three diffusion charger monitors (DC1, DC2, and NSAM). The SSA measured by BET analysis presented the largest scatter, but the values were found to be within the range of data obtained from the real-time monitors. Finally, the SSA normalized using the TEOM data was consistently lower than the SSA normalized with the TC and EC: the $SSA_{TEOM} < SSA_{TC} < SSA_{EC}$.

The particle number concentrations measured by the SMPS and portable CPC were also normalized in terms of the mass concentration of the aerosol obtained as total mass (TEOM) and TC and EC concentration (Figure 4, Figure S4). For each testing condition, the two instruments provided within error the same SNC results. With increasing engine load, the SNC values dropped drastically during both low and high mass concentration level testing. Table 4 summarizes the SNC values obtained by the combination of data presented in Tables 2 and 3. For each gram of TC, the number of particles counted by the SMPS varied from 4124×10^{12}–5925×10^{12} (5%) to 834×10^{12}–896×10^{12} (80%). Similar numbers were measured by the portable CPC.

DISCUSSION

DPM was analyzed in an aerosol chamber under different mass concentration levels and engine operating conditions to simulate aerosols present in underground noncoal mines. Three substantially different size distributions were obtained (Figure 1). The GMD of the aerosols varied from 66 to 135 nm (Figure 1) and were comparable with values previously reported by Bugarski et al. (2009) for aerosols generated by
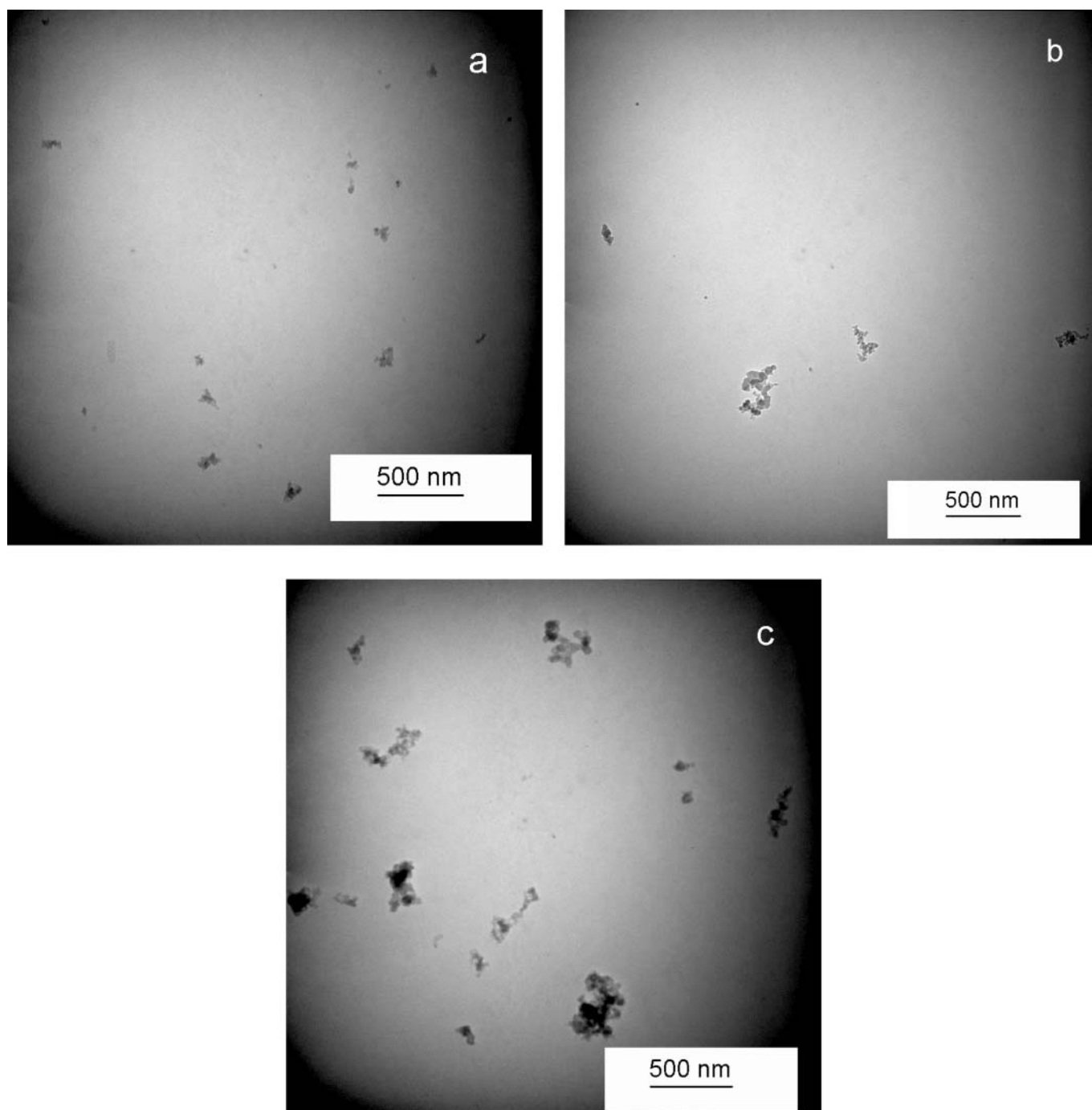
FIG. 2.   TEM photomicrographs of DPM generated in the Marple chamber under three engine load conditions: (a) 5%, (b) 30%, and (c) 80%.

untreated diesel exhaust in underground mines. Simultaneous measurement of mass, surface area, and number concentration were used to characterize the DPM aerosols. The average surface area concentration and number concentration values presented in this article compare well with the published data relative to diesel ultrafine particles or other nonengineered nanoparticles in occupational environments. The number con-

centration of diesel particles measured during a campaign on untreated exhaust in a laboratory mine was $(5.5–8.7) \times 10^5$ particles/cm^3 (Bugarski et al. 2009). The exposure of three occupational groups—bus drivers, parking garage attendants, and bus mechanics—to diesel particles was assessed with diffusion chargers and particle counters, with the surface area concentration varying between 60 and 150 μm^2/cm^3 and number

TABLE 3

Surface area and mass concentration of DPM aerosols measured with different instruments and techniques. Specific surface area (SSA) concentration obtained using the total real-time mass concentration (TEOM) and the surrogates (EC, TC) generally employed in mining environments to assess exposure to DPM

Engine load		5%	30%	80%	5%	30%	80%
Concentration level		Low	Low	Low	High	High	High
Surface area							
SMPS	$\mu m^2/cm^3$ [10^2]	44.5 ± 7.5	40.3 ± 7.1	52.1 ± 11.2	126.8 ± 19.1	249.3 ± 23.1	190.6 ± 22.5
NSAM	$\mu m^2/cm^3$ [10^2]	9.7 ± 1.9	6.4 ± 0.7	7.4 ± 2.3	34.7 ± 5.5	54.7 ± 4.6	38.2 ± 4.5
DC1	$\mu m^2/cm^3$ [10^2]	7.4 ± 1.1	5.8 ± 1.2	6.8 ± 1.6			
DC2	$\mu m^2/cm^3$ [10^2]	11.0 ± 1.6	9.9 ± 1.9	10.2 ± 2.4	27.4 ± 2.1	45.6 ± 4.1	
Mass Conc.							
TEOM	$\mu g/m^3$	67.5 ± 9.9	70.2 ± 11.2	118.2 ± 24.8	223.1 ± 35.6	462.3 ± 48.3	494.0 ± 65.8
TC	$\mu g/m^3$	55.2 ± 2.2	52.2 ± 2.6	90.8 ± 6.5	109.9 ± 6.4	344.6 ± 9.8	372.0 ± 23.9
EC	$\mu g/m^3$	31.2 ± 0.3	42.2 ± 0.3	88.8 ± 8.2	62.9 ± 3.7	273.6 ± 2.8	335.7 ± 6.4
SSA (TEOM)							
SMPS	m^2/g	66.1 ± 14.7	57.4 ± 13.6	44.1 ± 13.2	56.8 ± 12.4	53.9 ± 7.5	38.6 ± 6.8
NSAM	m^2/g	14.4 ± 3.6	9.1 ± 1.8	6.3 ± 2.4	15.6 ± 3.5	11.8 ± 1.6	7.7 ± 1.4
DC1	m^2/g	10.9 ± 2.3	8.3 ± 2.1	5.7 ± 1.8			
DC2	m^2/g	16.3 ± 3.4	14.1 ± 3.6	8.6 ± 2.7	12.3 ± 2.2	9.9 ± 1.4	
SSA (gravimetric)							
BET	m^2/g				25.7 ± 11.5	42.5 ± 25.1	28.8 ± 13.4
SSA (TC)							
SMPS	m^2/g	80.7 ± 13.0	77.3 ± 14.1	57.4 ± 12.9	115.3 ± 18.6	72.4 ± 7.1	51.2 ± 6.9
NSAM	m^2/g	17.6 ± 3.6	12.3 ± 1.5	8.2 ± 2.7	31.6 ± 5.4	15.9 ± 1.4	10.3 ± 1.4
DC1	m^2/g	13.4 ± 2.1	11.1 ± 2.3	7.5 ± 1.9			
DC2	m^2/g	20.0 ± 3.1	18.9 ± 3.8	11.3 ± 2.8	24.9 ± 2.4	13.2 ± 1.3	
SSA (EC)							
SMPS	m^2/g	142.9 ± 23.9	95.5 ± 16.7	58.7 ± 13.7	201.7 ± 32.5	91.1 ± 8.5	56.8 ± 6.8
NSAM	m^2/g	31.3 ± 6.9	15.2 ± 1.6	8.4 ± 2.8	55.3 ± 9.4	20.0 ± 1.7	11.4 ± 1.4
DC1	m^2/g	23.8 ± 3.5	13.7 ± 2.8	7.7 ± 1.9			
DC2	m^2/g	35.4 ± 5.3	23.4 ± 4.6	11.5 ± 2.9	43.6 ± 4.2	16.7 ± 1.5	

concentration between 0.25×10^5 and 1.5×10^5 particles/cm^3 (Ramachandran et al. 2005). The average number and surface area (DC) concentration of aerosols present in an automotive engine manufacturing center was $(1–2) \times 10^3$ $\mu m^2/cm^3$ and $5 \times 10^5–10^6$ particles/cm^3 respectively (Heitbrink et al. 2009).

As shown by Figures 3 and 4, a single metric does not define completely the DPM aerosols generated by an untreated exhaust. The DPM surface area, number concentration, and mass concentration are not related by defined univocal correlations. The surface area and number concentration per unit of mass (SSA and SNC) are not constant but they can vary up to twofold and fivefold, respectively. This implies that in mining environments the analysis of the exposure of miners to DPM will not be comprehensive if the monitoring is limited only to TC and EC. Unfortunately, only small instruments like diffusion chargers and portable counters can be employed in such an occupational environment on a regular basis.

To solve this assessment problem a new approach is proposed. The plots in Figures 3 and 4 show how the SSA and SNC results characterize the different operating conditions of the diesel engine and thus define the DPM aerosol at each condition. This is possible because the DPM aerosols evaluated, characterized only by the accumulation mode, have a variable GMD but a steady geometric standard deviation as previously reported (Harris and Maricq 2001). By using the SSA—obtained from the NSAM monitor and normalized by the TC or EC—as an input data it is possible to quantify the geometric surface area and the number concentration without any information related to the operating engine condition (Figure 5a and b). The proposed approach can be described in steps. Simultaneous collection of just NSAM and TC (EC), data are recorded and used to calculate the SSA—the input data-point. The specific geometric surface area and number concentration are then retroactively retrieved by using the presented plots (Figure 5a and b) and finally the
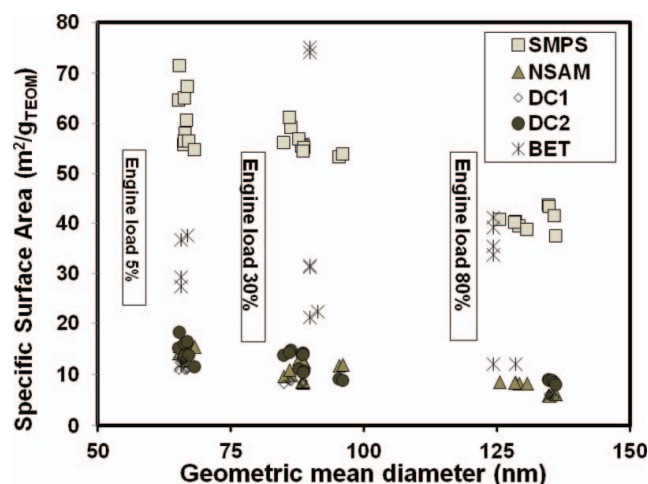
FIG. 3.   Specific surface area (SSA) of DPM aerosols generated in the Marple chamber under different conditions. The SSA is based on the mass concentration obtained by the TEOM. (Color figure available online.)
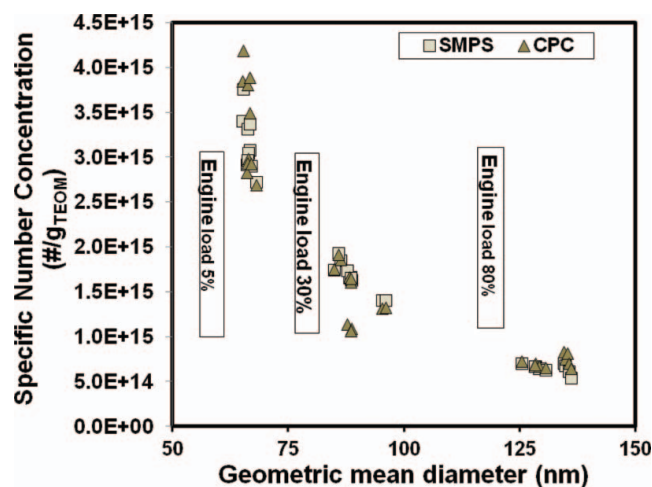

FIG. 4.   Specific number concentration (SNC) of DPM aerosols generated in the Marple chamber under different conditions. The SNC is based on the mass concentration obtained by the TEOM. (Color figure available online.)

electro-mobility surface area and the number concentration obtained by using the TC (EC) values measured. In the same way, the SNC—from a portable CPC and normalized by TC or EC–can be used to quantify the electro-mobility and lung deposited surface area (Figure 5c and d). Even if not reported, the active surface area (DC) can be used alternatively as an input or output data in this approach.

The application of the new approach to field data is based on the assumption that the plots in Figure 5 are valid for aerosols generated from diesel engines different than the one evaluated in this study. In this way, field collected SSA or SNC data can be used to quantify other properties not measured in the field. The validity of the assumption and proposed approach needs to be investigated and corroborated with further laboratory and field analysis in the future. While the nucleation mode is not considered in this approach, it is intuitive that any nucleation aerosol

occurrence would produce an extremely high value of SSA and SNC input data. If enhanced and enriched with the addition of data from different engine configurations, the new metric approach would have the benefit to reduce the number of simultaneous measurements. The approach is completely independent from the engine operating condition that is generally difficult information to obtain during field studies. Furthermore, it can potentially provide average values aerosols emitted by diesel engine under more realistic transient duty cycles or aerosol generated by multiple exhausts.

The approach described above is based on the measurements carried out by different monitors and measurements. For this reason, the measurements of the surface area employed in the new approach require some additional interpretation because each methodology is supposed to measure a different type of surface area. The surface area measured via off-line BET

TABLE 4
Specific number concentration (SNC) obtained using the mass concentration surrogates (EC, TC) generally employed in mining environments to assess exposure to DPM

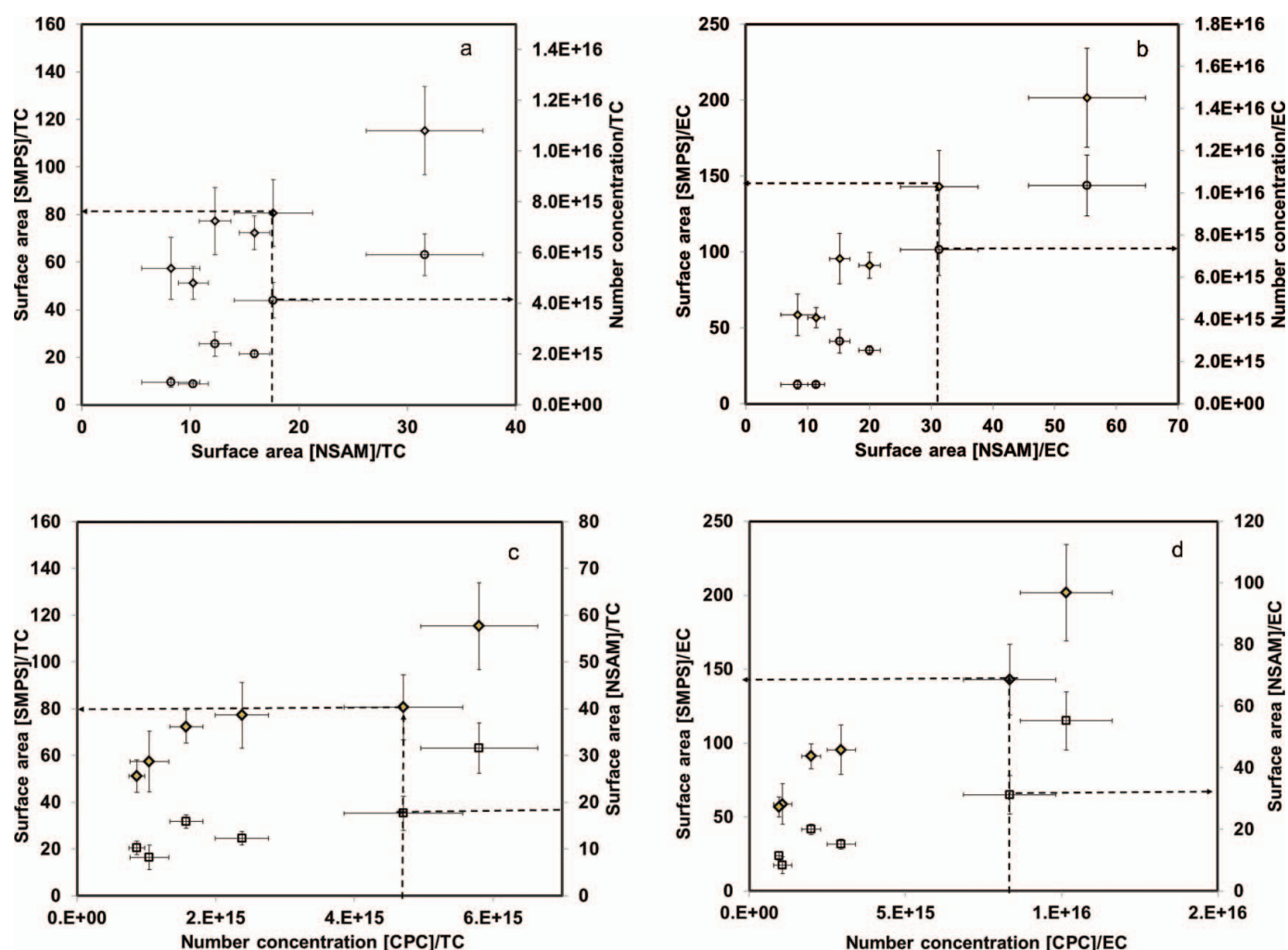| Engine load Concentration level		5% Low	30% Low	80% Low	5% High	30% High	80% High
				$SNC\ (TEOM)—10^{14}$			
SMPS	#/g	33.7 ± 7.4	17.8 ± 4.4	6.9 ± 2.1	29.2 ± 5.9	15.0 ± 1.9	6.3 ± 1.1
CPC	#/g	38.5 ± 8.9	17.7 ± 3.9	8.0 ± 2.7	28.6 ± 5.9	11.7 ± 2.1	6.5 ± 1.1
				$SNC\ (TC)—10^{14}$			
SMPS	#/g	41.2 ± 7.0	23.9 ± 4.7	8.9 ± 2.0	59.2 ± 8.2	20.1 ± 1.7	8.3 ± 1.2
CPC	#/g	47.1 ± 8.6	23.8 ± 3.8	10.4 ± 2.8	58.0 ± 8.4	15.8 ± 2.3	8.6 ± 1.1
				$SNC\ (EC)—10^{14}$			
SMPS	#/g	70.2 ± 12.1	29.6 ± 567	9.2 ± 2.1	103.6 ± 14.4	25.3 ± 2.1	9.2 ± 1.2
CPC	#/g	83.4 ± 14.8	29.4 ± 4.5	10.7 ± 2.9	101.5 ± 14.7	19.8 ± 2.9	9.5 ± 1.1

FIG. 5. The new metric approach presented with different SSA and SNC inputs data: (a) specific NSAM surface area (TC); (b) specific NSAM surface area (EC); (c) specific number concentration (TC); and (d) specific number concentration (EC). (Color figure available online.)

technique showed a very high scatter pattern and this presents an issue for comparing these data with the real-time technique results. The interaction of different DPM particles with the microfibers of the TX40 filters might have an influence in the absorption technique. In addition the possible degassing of the fibers in the filter media in the preparation for the BET analysis might have occurred. The three real-time techniques provided substantially different values of the DPM surface area concentration (Table 3). In theory, the surface area measured by the SMPS analyzer and corrected by the IA method represents the geometric surface area of the DPM aggregates. The assumption is that all the primary particles are equally exposed to the surrounding gas: the aggregates need to be linear-chain assumption with a low fractal dimension. Recently, Ku and Kulkarni (2012) showed that the geometric surface area of aggregates is underestimated by the IA method applied to mobility analysis when the chains have a fractal dimension of 2.37–2.63. Because no statistical morphology analysis was carried out in this study,

the SMPS surface area can be considered only an estimation of geometric surface area. By processing the recorded data, The NSAM signal for a single particle was found to be proportional with the mobility diameter to a power of 1.17. Studies on single NaCl particles (Jung and Kittelson 2005) and urban airborne nanoparticles (Ntziachristos et al. 2007) determined the NSAM proportionality as $d^{1.13}$ and $d^{1.258}$, respectively. Wilson et al. (2007) used the NSAM, previously known as EAD, for the measurement of urban particles from 3 to 500 nm and found the lung-deposited surface area and the NSAM signal to be proportional to $d^{1.1-1.6}$ and $d^{1.25}$, respectively. For this reason, the NSAM measured the lung (alveolar) deposit surface area of different DPM particles present in the aerosol chamber. For the two diffusion charger a proportionality of $d^{1.34}$ (DC1) and $d^{1.44}$ (DC2) was found. The values are consistent with previous studies: Ku and Maynard (Ku and Maynard 2005) found a proportionality of 1.5 for similar diffusion chargers when exposed to monodisperse silver nanoparticles for particle sizes from 80

to 200 nm. From a theoretical perspective, the output of the DCs evaluated in this study agrees with the Fuchs surface area, which is proportional to $d^{1.39}$ (Fuchs 1963). The surface area measured by the two DCs in Table 3 was therefore the active surface area of the DPM particles present in the exposure chamber.

SUMMARY

The presence of DPM in underground mines leads to occupational exposure to ultrafine particles. While the mass concentration of an aerosol is commonly used as the only metric in occupational exposure assessment studies, surface and number concentration have received increasing attention for characterizing the exposure to particles below 100 nm. Because there is still no certainty on which metric better characterizes the aerosols in the interpretation of the toxicity data, the measurement of more than one metric should be carried out. In addition, the complexity of the surface area measurement for DPM suggests the use of different real-time and off-line methods.

This study proved that a single metric is not sufficient to fully characterize DPM particles. The surface area and number concentrations of the particles per unit of mass, and particularly per unit of TC were not constant but varied from 2 to 10 times, respectively, under different engine operating conditions. This finding implies that the mass content alone of TC or EC in underground samples does not provide complete information on worker exposure in this workplace. To solve this exposure assessment problem a new approach was proposed. The approach entails combining two field-based measurements and calculating the SSA to retroactively obtain other physical characteristics/metrics of the DPM aerosols. The SNC can be also used instead of the SSA. The new approach is independent from the engine operating conditions and it has the potential to be used for the assessment of aerosols generated by more realistic transient cycles and multiple untreated exhausts.

Future works should challenge the new metric approach with different diesel engines and real underground mine aerosols. In addition, the evaluation of DPM particles emitted by diesel engines equipped with aftertreatment control technologies should be considered.

REFERENCES

71 Fed. Reg. 28924 (2006). Mine Safety and Health Administration: 30 CFR 57: Diesel Particulate Matter Exposure of Underground Metal and Nonmetal Miners. Limit on Concentration of Diesel Particulate Matter, Code of Federal Regulations, Washington, DC: U.S. Government Printing Office, Office of the Federal Register.

Alfoldy, B., Giechaskiel, B., Hofmann, W., and Drossinos, Y. (2009). Size-distribution Dependent Lung Deposition Of Diesel Exhaust Particles. *J. Aerosol Sci.*, 40:652–663.

Asbach, C., Fissan, H., Stahlmecke, B., Kuhlbusch, T. A. J., and Pui, D. Y. H. (2009). Conceptual Limitations and Extensions of Lung-deposited Nanoparticle Surface Area Monitor (NSAM). *J. Nanopart. Res.*, 11:101–109.

Balbus, J. M., Maynard, A. D., Colvin, V. L., Castranova, V., Daston, G. P., Denison, R. A., et al. (2007). Meeting Report: Hazard Assessment for Nanoparti-

cles - Report from an Interdisciplinary Workshop. *Environ. Health Perspect.*, 115:1654–1659.

Benbrahim-Tallaa, L., Baan, R. A., Grosse, Y., Lauby-Secretan, B., El Ghissassi, F., Bouvard, V., et al. (2012). Carcinogenicity of Diesel-engine and Gasoline-engine Exhausts and Some Nitroarenes. *Lancet Oncol.*, 13:663–664.

Birch, M. E. (2002). Occupational Monitoring of Particulate Diesel Exhaust by NIOSH Method 5040. *Appl. Occup. Environ. Hyg.*, 17:400–405.

Brown, D. M., Wilson, M. R., MacNee, W., Stone, V., and Donaldson, K. (2001). Size-dependent Proinflammatory Effects of Ultrafine Polystyrene Particles: A Role for Surface Area and Oxidative Stress in the Enhanced Activity of Ultrafines. *Toxicol. Appl. Pharmacol.*, 175:191–199.

Brunauer, S., Emmett, P. H., and Teller, E. (1938). Adsorption of Gases in Multimolecular Layers. *J. Ann. Chem. Soc.*, 60:309–319.

Bugarski, A. D., Schnakenberg, G. H., Hummer, J. A., Cauda, E., Janisko, S. J., and Patts, L. D. (2009). Effects of Diesel Exhaust Aftertreatment Devices on Concentrations and Size Distribution of Aerosols in Underground Mine Air. *Environ. Sci. Technol.*, 43:6737–6743.

Bugarski, A. D., Schnakenberg, G. H., Noll, J. D., Mischler, S. E., Patts, L. D., Hummer, J. A., et al. (2006). Effectiveness of selected diesel particulate matter control technologies for underground mining applications: Isolated zone study, 2003, Report of Investigations 9667, 2006–126, U.S. Department of Health and Human Services, Centers for Disease Control and Prevention and National Institute for Occupational Safety and Health, eds., Cincinnati, Ohio.

Chung, A., Lall, A. A., and Paulson, S. E. (2008). Particulate Emissions by a Small Non-road Diesel Engine: Biodiesel and Diesel Characterization and Mass Measurements Using the Extended Idealized Aggregates Theory. *Atmos. Environ.*, 42:2129–2140.

Evans, D. E., Ku, B. K., Birch, M. E., and Dunn, K. H. (2010). Aerosol Monitoring during Carbon Nanofiber Production: Mobile Direct-Reading Sampling. *Ann. Occup. Hyg.*, 54:514–531.

Fissan, H., Neumann, S., Trampe, A., Pui, D. Y. H., and Shin, W. G. (2007). Rationale and Principle of an Instrument Measuring Lung Deposited Nanoparticle Surface Area. *J. Nanopart. Res.*, 9:53–59.

Fubini, B., Ghiazza, M., and Fenoglio, I. (2010). Physico-chemical Features of Engineered Nanoparticles Relevant to their Toxicity. *Nanotoxicology*, 4:347–363.

Fuchs, N. A. (1963). On the Stationary Charge Distribution on Aerosol Particles in a Bipolar Ionic Atmosphere. *Geofisica Pura E Applicata*, 56:185–193.

Giechaskiel, B., Alfoldy, B., and Drossinos, Y. (2009). A Metric for Health Effects Studies of Diesel Exhaust Particles. *Aerosol Sci.*, 40:639–651.

Harris, S. J., and Maricq, M. M. (2001). Signature Size Distributions for Diesel and Gasoline Engine Exhaust Particulate Matter. *J. Aerosol Sci.*, 32:749–764.

Heitbrink, W. A., Evans, D. E., Ku, B. K., Maynard, A. D., Slavin, T. J., and Peters, T. M. (2009). Relationships Among Particle Number, Surface Area, and Respirable Mass Concentrations in Automotive Engine Manufacturing. *J. Occup. Environ. Hyg.*, 6:19–31.

Hesterberg, T. W., Long, C. M., Lapin, C. A., Hamade, A. K., and Valberg, P. A. (2010). Diesel Exhaust Particulate (DEP) and Nanoparticle Exposures: What do DEP Human Clinical Studies Tell Us About Potential Human Health Hazards Of Nanoparticles? *Inhal. Toxicol.*, 22:679–694.

Jung, H. J., and Kittelson, D. B. (2005). Characterization of Aerosol Surface Instruments in Transition Regime. *Aerosol Sci. Technol.*, 39:902–911.

Karakoti, A. S., Hench, L. L., and Seal, S. (2006). The Potential Toxicity of Nanomaterials - The Role of Surfaces. *Jom*, 58:77–82.

Kittelson, D. B. (1998). Engines and Nanoparticles: A Review. *J. Aerosol Sci.*, 29:575–588.

Ku, B. K. (2010). Determination of the Ratio of Diffusion Charging-based Surface Area to Geometric Surface Area for Spherical Particles in the Size Range of 100–900 nm. *J. Aerosol Sci.*, 41:835–847.

Ku, B. K., and Kulkarni, P. (2012). Comparison of Diffusion Charging and Mobility-based Methods for Measurement of Aerosol Agglomerate Surface Area. *J. Aerosol Sci.*, 47:100–110.

Ku, B. K., and Maynard, A. D. (2005). Comparing Aerosol Surface-area Measurements of Monodisperse Ultrafine Silver Agglomerates by Mobility Analysis, Transmission Electron Microscopy and Diffusion Charging. *J. Aerosol Sci.*, 36:1108–1124.

Lall, A. A., and Friedlander, S. K. (2006). On-line Measurement of Ultrafine Aggregate Surface Area and Volume Distributions by Electrical Mobility Analysis: I. Theoretical Analysis. *J. Aerosol Sci.*, 37:260–271.

Marple, V. A., and Rubow, K. L. (1983). An Aerosol Chamber for Instrument Evaluation and Calibration. *Am. Ind. Hyg. Assoc. J.*, 44:361–367.

Mathis, U., Mohr, M., Kaegi, R., Bertola, A., and Boulouchos, K. (2005). Influence of Diesel Engine Combustion Parameters on Primary Soot Particle Diameter. *Environ. Sci. Technol.*, 39:1887–1892.

Maynard, A., and Jensen, P. (2001). *Aerosol Measurement in the Workplace*, in *Aerosol Measurement: Principles, techniques and applications*, P. A. Baron, and K. Willeke, eds. Wiley Interscience, New York, pp. 779–799.

Maynard, A., and Kuempel, E. (2005). Airborne Nanostructured Particles and Occupational Health. *J. Nanopart. Res.*, 7:587–614.

Maynard, A. D., and Aitken, R. J. (2007). Assessing Exposure to Airborne Nanomaterials: Current Abilities and Future Requirements. *Nanotoxicology*, 1:26–41.

Miller, A., Frey, G., King, G., and Sunderman, C. (2010). A Handheld Electrostatic Precipitator for Sampling Airborne Particles and Nanoparticles. *Aerosol Sci. Technol.*, 44:417–427.

Monteiller, C., Tran, L., MacNee, W., Faux, S., Jones, A., Miller, B., et al. (2007). The Pro-inflammatory Effects of Low-toxicity Low-solubility Particles, Nanoparticles and Fine Particles, on Epithelial Cells In Vitro: The Role of Surface Area. *Occup. Environ. Med.*, 64:609–615.

National Institute for Occupational Safety and Health NIOSH and CDC (1988). Carcinogenic effects of exposure to diesel exhaust, Current Intelligence Bulletin 50, DHHH Publication #88–116, Atlanta.

Noll, J., and Birch, M. E. (2008). Effects of Sampling Artifacts on Occupational Samples of Diesel Particulate Matter. *Environ. Sci. Technol.*, 42:5223–5228.

Noll, J. D., Timko, R. J., McWilliams, L., Hall, P., and Haney, R. (2005). Sampling Results of the Improved SKC Diesel Particulate Matter Cassette. *J. Occup. Environ. Hyg.*, 2:29–37.

Ntziachristos, L., Giechaskiel, B., Ristimaki, J., and Keskinen, J. (2004). Use of a Corona Charger for the Characterisation of Automotive Exhaust Aerosol. *J. Aerosol Sci.*, 35:943–963.

Ntziachristos, L., Polidori, A., Phuleria, H., Geller, M. D., and Sioutas, C. (2007). Application of a Diffusion Charger for the Measurement of Particle Surface Concentration in Different Environments. *Aerosol Sci. Technol.*, 41:571–580.

Oberdorster, G., Oberdorster, E., and Oberdorster, J. (2005). Nanotoxicology: An Emerging Discipline Evolving from Studies of Ultrafine Particles. *Environ. Health Perspect.*, 113:823–839.

Park, K., Kittelson, D. B., and McMurry, P. H. (2004). Structural Properties of Diesel Exhaust Particles Measured by Transmission Electron Microscopy (TEM): Relationships to Particle Mass and Mobility. *Aerosol Sci. Technol.*, 38:881–889.

Pauluhn, J. (2009). Retrospective Analysis of 4-week Inhalation Studies in Rats with Focus on Fate and Pulmonary Toxicity of Two Nanosized Aluminum Oxyhydroxides (Boehmite) and Pigment-Grade Iron Oxide (Magnetite): The Key Metric of Dose is Particle Mass and Not Particle Surface Area. *Toxicology*, 259:140–148.

Ramachandran, G., Paulsen, D., Watts, W., and Kittelson, D. (2005). Mass, Surface Area and Number Metrics in Diesel Occupational Exposure Assessment. *J. Environ. Monit.*, 7:728–735.

Sager, T. M., and Castranova, V. (2009). Surface Area of Particle Administered Versus Mass in Determining the Pulmonary Toxicity of Ultrafine and Fine Carbon Black: Comparison to Ultrafine Titanium Dioxide. *Particle and Fibre Toxicology*, 6(15):1–12.

Sager, T. M., Kommineni, C., and Castranova, V. (2008). Pulmonary Response to Intratracheal Instillation of Ultrafine Versus Fine Titanium Dioxide: Role of Particle Surface Area. *Particle and Fibre Toxicology*, 5.

Schulte, P., Murashov, V., Zumwalde, R., Kuempel, E., and Geraci, C. (2010). Occupational Exposure Limits for Nanomaterials: State of the Art. *J. Nanopart. Res.*, 12:1971–1987.

Swanson, J., Kittelson, D., Pui, D., and Watts, W. (2010). Alternatives to the Gravimetric Method for Quantification of Diesel Particulate Matter near the Lower Level of Detection. *J. Air Waste MA.*, 60:1177–1191.

Tran, C. L., Buchanan, D., Cullen, R. T., Searl, A., Jones, A. D., and Donaldson, K. (2000). Inhalation of Poorly Soluble Particles. II. Influence of Particle Surface Area on Inflammation and Clearance. *Inhal. Toxicol.*, 12:1113–1126.

Walton, W. H., and Vincent, J. H. (1998). Aerosol Instrumentation in Occupational Hygiene: An Historical Perspective. *Aerosol Sci. Technol.*, 28:417–438.

Wang, C.-S., and Friedlander, S. K. (2007). Determination of Surface Area and Volume of Nanoparticle Aggregates Deposited in the Human Respiratory Tract Using DMA Data. *J. Aerosol Sci.*, 38:980–987.

Wilson, W. E., Stanek, J., Han, H. S., Johnson, T., Sakurai, H., Pui, D. Y. H., et al. (2007). Use of the Electrical Aerosol Detector as an Indicator of the Surface Area of Fine Particles Deposited in the Lung. *J. Air Waste MA.*, 57:211–220.

Wittmaack, K. (2007). In Search of the Most Relevant Parameter for Quantifying Lung Inflammatory Response to Nanoparticle Exposure: Particle Number, Surface Area, or What? *Environ. Health Perspect.*, 115:187–194.

Woo, K. S., Chen, D. R., Pui, D. Y. H., and Wilson, W. E. (2001). Use of Continuous Measurements of Integral Aerosol Parameters to Estimate Particle Surface Area. *Aerosol Sci. Technol.*, 34:57–65.